Clinical and Experimental Medicine (2025) 25:65
https://doi.org/10.1007/s10238-025-01572-8

RESEARCH

YY1-mediated DUXAP8 facilitates HCC progression via modulating DEPDC1 expression

Yi Cui[1] · Yong Sun[2] · Na Liang[3,4] · Chuan Tian[3,4]

Received: 16 December 2024 / Accepted: 17 January 2025

Abstract

The long noncoding RNA DUXAP8 has been implicated in the progression of various malignancies, including hepatocellular carcinoma (HCC). Although there is increasing evidence of DUXAP8's role in tumor biology, the exact mechanisms by which it affects the development and treatment of HCC are still unclear. Previous studies have suggested a potential link between DUXAP8 expression and disease progression, necessitating further investigation into its roles and underlying mechanisms. To clarify how DUXAP8 is involved in HCC, we measured its expression in HCC cell lines and tissues from patients. We utilized in vitro assays to evaluate the effects of DUXAP8 on tumor cell proliferation and metastasis. Additionally, we examined the regulatory relationships between DUXAP8, YY1, and DEPDC1 using RNA immunoprecipitation and luciferase reporter assays to investigate their functional mechanisms. Our findings demonstrated that DUXAP8 is frequently upregulated in HCC specimens and that its overexpression significantly enhances both the proliferation and metastatic capability of HCC cells. Importantly, the expression levels of DUXAP8, YY1, and DEPDC1 showed correlations with clinical parameters such as disease stage and histopathological characteristics. Mechanistically, we uncovered that YY1 regulates DUXAP8, which, in turn, modulates DEPDC1 expression through a dual mechanism involving the sponging of miR-7-5p and the stabilization of DEPDC1 mRNA facilitated by HNRNPF. Our study identifies DUXAP8 as a pivotal factor in the proliferation and metastasis of HCC, acting through the DUXAP8/miR-7-5p and DUXAP8/HNRNPF pathways to regulate DEPDC1 expression. These findings indicate that targeting DUXAP8 could be a new therapeutic strategy for treating HCC. Further research in both preclinical and clinical settings is needed to evaluate its potential as a biomarker and therapeutic target in liver cancer management.

Keywords Hepatocellular carcinoma · YY1 · DUXAP8 · MiR-7-5p · HNRNPF · DEPDC1

Background

Hepatocellular carcinoma (HCC) is one of the most common malignant tumors worldwide and is most prevalent in China, where survivorship after five years is very low [1, 2]. The opportunity for radical resection is frequently lost in patients with HCC due to local progression and distant metastases [3, 4]. Therefore, it is crucial to elucidate the molecular mechanisms underlying the development of HCC.

DEP domain containing 1 (DEPDC1) is a novel oncogene upregulated in HCC and is believed to be an innovative cancer diagnostic marker as well as a molecular target for the development of novel therapeutic drugs or vaccines targeting cancer peptides [5, 6]. Studies have indicated that increased DEPDC1 expression is linked to a poor prognosis in patients with HCC, and the regulation of HCC proliferation and metastasis is attributed to DEPDC1[7]. Long

Yi Cui and Yong Sun have contributed equally to this work.

✉ Chuan Tian
teechuan2015@126.com

1 Clinical Research Center, The Affiliated Hospital of Guizhou Medical University, Guiyang, Guizhou, China

2 Department of Hepatobiliary Gastrointestinal Surgery, People's Hospital of YanHe, Tongren, China

3 Department of Oncology, The Affiliated Hospital of Guizhou Medical University, Guiyang, China

4 Department of Oncology, The Affiliated Cancer Hospital of Guizhou Medical University, Guiyang, China

Published online: 24 February 2025

noncoding RNAs (LncRNAs) associated with DEPDC1 are involved in cancer [8]. Tian et al. suggested that modulation of DEPDC1 expression by Linc-ROR promotes the advancement and angiogenic activity in HCC [7]. Moreover, lncRNA activation is a crucial factor in the development of hepatic oncogenesis and tumor cell progression [9]. Several studies have shown that LncRNAs regulate HCC progression through DEPDC1. Therefore, further clarification of the roles of DEPDC1 and LncRNAs in HCC progression is required.

YY1 can interact with lncRNA, regulate gene expression and cell function. Its expression level shows a positive correlation with certain lncRNA, which can promote cell proliferation, differentiation and survival. It can also form a complex to regulate the expression of downstream genes [10, 11]. YY1 is highly expressed in HCC and closely related to the malignancy degree and prognosis, and may promote the occurrence and development of HCC by regulating various processes [12]. An in-depth study of its interaction mechanism and role in HCC can provide new targets and strategies for diagnosis and treatment.

Increasing evidence suggests that LncNRAs, comprising RNA molecules exceeding 200 nucleotides in length that lack protein-coding capacity, play diverse roles in cancer progression. This highlights their potential use as diagnostic biomarkers and therapeutic targets [13, 14]. The lncRNA double homeobox A pseudogene 8 (DUXAP8), an lncRNA originating from a pseudogene, is overexpressed in various human cancers. It has been suggested as a promising pan-cancer biomarker for both diagnostic and prognostic applications [15]. Previous research has demonstrated that upregulation of DUXAP8 expression is associated with an unfavorable prognosis, serves as a prognostic biomarker, and stimulates HCC cell progression [16]. However, the precise mechanisms underlying the oncogenic properties of DUXAP8 remain unclear.

This study investigated the potential involvement of DUXAP8 in HCC and presented evidence that DUXAP8 upregulates the expression of DEPDC1, thereby promoting HCC progression. Our findings demonstrated that DUXAP8 functions as a competing endogenous RNA (ceRNA) to modulate the activity of DEPDC1, resulting in enhanced DEPDC1 mRNA stability through the facilitation of DEPDC1-HNRNPF mRNA interaction.

Materials and methods

Visualization and processing of data

The Cancer Genome Atlas (TCGA) (https://portal.gdc.cancer.gov/) databases [17] was utilized to conduct an analysis of the expression levels of YY1 and DEPDC1 in all normal and HCC tissues, The genes that exhibited differential expression were obtained from TCGA. RNA sequencing profiles from TCGA were downloaded for TCGA-LIHC clinical observations. To conduct profiling RNA sequencing data, the software GraphPad 9.0 was utilized.

Clinical specimens

Between July 2018 and December 2022, a cohort of 32 HCC tissues and their corresponding nontumor tissues were procured from the Affiliated Hospital of Guizhou Medical University. Prior to surgery, none of the patients underwent chemotherapy or radiotherapy. This study was approved by the hospital ethics committee, and prior to participation, informed consent was obtained from each patient.

Cell culture and antibodies

The Shanghai Cell Bank (Shanghai, China) provided the Huh7 and Hep3B and cell line THLE-3 derived from a normal liver. The cells were subjected to incubation at 37 °C by a humidified incubator containing 5% CO_2, and cell lines were confirmed to be devoid of mycoplasma contamination.

In this study, the primary antibodies employed were rabbit antihuman DEPDC1 (dilution 1:1000; cat. no. PA5-34864; Thermo Fisher Scientific, Inc); and mouse anti-HNRNPF (dilution 1:1000; cat. no. 67701-1-Ig; ProteinTech Group, Inc); mouse anti-lgG (dilution 1:1000; cat. no. #5946; CST); rabbit anti-N-cadherin (dilution 1:1000; cat. no. ab202030; Abcam); rabbit anti-Vimentin (dilution 1:1000; cat. no. ab217673; Abcam); mouse antihuman GAPDH (dilution 1:5000; cat. no. #97166; CST); rabbit anti-Ago2 (dilution 1:1000; cat. no. 10686-1-AP; ProteinTech Group, Inc); Secondary antibodies included rabbit anti-goat IgG (H + L) (dilution 1:5000; cat. no. SA00001-4; ProteinTech Group, Inc) and goat anti-mouse (dilution 1:5000; cat. no.SA00001-1; ProteinTech Group, Inc).

Cell transfection

Genechem (Shanghai, China) designed and synthesized Lentivirus expressing shDUXAP8 (Lv-shDUXAP8) or shDEPDC1 (Lv-shDEPDC1), as well as Lentivirus overexpressing DUXAP8 (Lv-DUXAP8) and Lv-DEPDC1. Stable cell lines (Hep3B and Huh7) were generated via lentiviral transduction. Corves (Nanjing, China) designed and synthesized siRNA targeting HNRNPF, as well as plasmids for HNRNPF and DEPDC1 overexpression. The miR-7-5p mimic, inhibitor and negative controls were procured from RiboBio (Guangzhou, China). Using Lipofectamine 2000 reagent (Invitrogen) in accordance with the guidelines of manufacturer.

qRT-PCR

The StepOne Plus RT PCR System (Thermo, USA) was utilized to conduct qRT-PCR, employing SYBR Green (Vazyme, China) as the detection method after total RNA extraction using Trizol Reagent (Sigma, St. Louis, MO, USA). Utilizing the 2-ΔΔCT method by GAPDH and U6 as an internal parameter, we repeat three biological replicates of comparative qRT-PCR. This investigation used a variety of primers, as shown in Table 1.

Western blot

The cells underwent lysis in RIPA lysis buffer, and the quantification of protein concentrations was performed through employment of the BCA method. The membranes were subjected to incubation with primary and secondary antibodies. The protein bands were detected through the utilization of Detection by enhanced chemiluminescence (Pharmacia, Piscataway, NJ, USA). All Western blots were repeated at least 3 times. The density of the immunoreactive bands was quantified using ImageJ software.

Cytosolic and nuclear fractionation

The Hep3B and Huh7 cells underwent two washes with PBS and were subsequently subjected to incubation with hypotonic buffer at 0 °C for a duration of 10 min. The cells underwent centrifugation at a force of 5000 × g for a duration of 5 min, resulting in the collection of the supernatants. The resuspension of pellets was carried out in a nucleus resuspension buffer comprising of 20 mM HEPES, pH 7.9, 400 mM NaCl, 1 mM EDTA, 1 mM EGTA, 1 mM DTT, and 1 mM PMSF for a duration of 30 min. The samples underwent centrifugation at 12,000 × g for a duration of 10 min, following which the nuclear fraction was obtained by collecting the supernatant. During qRT-PCR analysis, GAPDH and U6 mRNA were employed as markers for the cytosolic and nuclear compartments, respectively.

Table 1 Sequences of PCR primers used in this study

Names	Primer Sequence (5′–3′)
lncRNA DUXAP8: Forward	ACCCAAACACTAATTGTAGACT
lncRNA DUXAP8: Reverse	TGTCTGGGAGACTGCTTACA
YY1: Forward	ACGGCTTCGAGGATCAGATTC
YY1: Reverse	TGACCAGCGTTTGTTCAATGT
miR-7-5p: Forward	UGGAAGACUAGUGAUUUU GUUGU
miR-7-5p: Reverse	UUUGUACUACACAAAAGUACUG
HNRNPF: Forward	AATTGTGCCAAACGGGATCAC
HNRNPF: Reverse	GTGTTTCCCTAGAGCCTTCTCA
DEPDC1: Forward	CTCGTAGAACTCCTAAAAGGC ATG
DEPDC1: Reverse	CAACATCTTCCTGGCTTAGTTCTC
GAPDH: Forward	GGAGCGAGATCCCTCCAAAAT
GAPDH: Reverse	GGCTGTTGTCATACTTCTCATGG
U6: Forward	CTCGCTTCGGCAGCACA
U6: Reverse	AACGCTTCACGAATTTGCGT
Vimentin: Forward	AGGCAAAGCAGGAGTCCACTGA
Vimentin: Reverse	ATCTGGCGTTCCAGGGACTCAT
N-cadherin: Forward	CCTCCAGAGTTTACTGCCATGAC
N-cadherin: Reverse	GTAGGATCTCCGCCACTGATTC

Luciferase reporter assay

The pmirGLO, pmirGLO-WT, or pmirGLO-MUT (Promega, Madison, WI, USA) for DUXAP8 and DEPDC1 were co-transfected with miR-7-5p mimic or the negative control (mimic NC) into Hep3B and Huh7 cells by using Lipofectamine-mediated gene transfer. The Dual Luciferase Reporter Gene system (Promega) was employed to detect luciferase activities 48 h post-transfection, in accordance with the manufacturer's instructions.

RNA pull-down assay

To generate probe-coated beads, streptavidin magnetic beads (RioBio, China) were incubated with a biotin-labeled DUXAP8, the DEPDC1 3′UTR and the control probe (100 pmol) (RiboBio, China) at room temperature for 2 h. The lysates obtained from Hep3B and Huh7 cells were subjected to an overnight incubation with probe-coated beads at a temperature of 4 °C. Subsequently, the beads underwent a washing procedure, followed by the analysis of the extracted miRNA through qRT-PCR.

RNA immunoprecipitation

The Magna RIP RNA-Binding Protein Immunoprecipitation Kit (Millipore, USA) was utilized to incubate anti-HNRNPF, anti-IgG and anti-AGO2 by magnetic beads for a duration of 30 min at room temperature, following the manufacturer's instructions. Subsequently, the antibody-bead complexes were subjected to an overnight incubation at 4 °C with cell lysates obtained from Hep3B and Huh7 cells. The RNAs that were bound were subjected to elution, followed by reverse transcription to cDNA, and ultimately detected through qRT-PCR.

Chromatin immunoprecipitation assay

ChIP assay was performed using EZ-Magna ChIP A/G (17–10086, Upstate, Millipore, MA, USA) kit according to the manufacturer's instructions. The cells were immobilized

using a 1% formaldehyde solution, followed by quenching with glycine by the ChIP assay (Millipore, USA). The resulting crosslinked chromatin was subsequently fragmented to a size range of 200–1000 bp through sonication. The lysates were subjected to incubation with the respective antibodies and Magna ChIP Protein G Magnetic beads at a temperature of 4 °C for an extended period of time with mild agitation. The ChIP complexes were subjected to elution and subsequent analysis via qRT-PCR. The resulting data were computed utilizing the 2-ΔΔCT method.

CCK-8 assay

In this experiment, cells were sown at a density of 2.0×10^3cells/well in 96-well plates. The assessment of cell proliferation was conducted in accordance with CCK-8 assay (Dojindo, Japan). For the subsequent five days, added to each well by a mixture of 10 µl of CCK-8 reagent and 90 µl of medium. Following a 2-h incubation period at 37 °C under light-excluded conditions, it quantified in each well using a microplate reader at 450 nm.

EdU assay

The Zeiss fluorescence photomicroscope (Carl Zeiss, Oberkochen, Germany) was utilized to obtain the results, which were subsequently quantified by counting a minimum of five randomly selected fields utilizing the EdU kit (Roche, Indianapolis, IN, USA).

Transwell assay

The Transwell chamber (Corning, NY, USA) was utilized to conduct migration assays. The upper chambers were utilized for the placement of cells. A medium comprising 10% serum was introduced into the lower chambers. Following a 24-h incubation period and subsequent fixation with 4% formaldehyde, the cells that had migrated to the lower surface were subjected to staining with 0.1% crystal violet. The cells were visualized and enumerated utilizing an Olympus microscope.

Statistical analysis

The experiments were conducted independently on a minimum of three occasions, and statistical analyses were carried out utilizing GraphPad Prism 9.0 (GraphPad, La Jolla, CA, USA). The statistical significance of the variances between experimental groups was assessed through the utilization of Student's t-tests, while differences among multiple groups were evaluated via one-way ANOVA. The presentation of quantitative data is in the form of mean ± SD (standard deviation) derived from triplicate measurements. A statistically significant difference was deemed to exist if $*p < 0.05$, $**p < 0.01$, or $***p < 0.001$.

Results

DUXAP8 expression is increased in HCC

R software was used to analyze the expression of YY1 and DEPDC1 in datasets obtained from TCGA-LIHC datasets to identify potential LncRNAs implicated in the progression of HCC (Fig. 1A). The TCGA-LIHC database was used to perform a correlation analysis between YY1 and DEPDC1, which yielded a statistically significant and positive correlation (cor = 0.516, $P = 3.337e{-}30$) (Fig. 1B). The Venn diagram showed that both YY1 and DEPDC1 shared 45 LncRNAs ($R > 0.3$, $P < 0.001$) (Fig. 1C). We then performed differential expression profiling of 45 LncRNAs, showing that seven LncRNAs (LogFC > 2, FDR < 0.05) (Fig. 1D). Next, we constructed a risk signature for HCC using univariate Cox regression and selected the lncRNA DUXAP8 with the highest expression (hazard rate = 1.861 and area under the curve = 0.680; Table 2).

Subsequently, we examined the expression of DUXAP8 in both hepatocellular carcinoma cells and tissues. The expression levels of DUXAP8 were compared between normal and HCC tissues using the TCGA-LIHC database (Fig. 1E). The expression of DUXAP8 was significantly elevated in HCC tissues compared to normal tissues, and a decreased level of DUXAP8 expression was indicative of a favorable prognosis (Fig. 1F). To further support these results, reverse transcription polymerase chain reaction was used to analyze our study population, which revealed a significant upregulation of DUXAP8 expression in HCC specimens compared to that in liver tissues ($P < 0.001$) (Fig. 1G). Furthermore, the two HCC cell lines exhibited elevated levels of DUXAP8 expression compared to the THLE-3 normal liver cell line (Fig. 1H). Taken together, these findings suggest that the expression of DUXAP8 is increased in HCC cells.

The activation of DUXAP8 expression in HCC cells is facilitated by YY1

In light of the observed overexpression of DUXAP8 in HCC, our subsequent efforts were directed toward elucidating the potential mechanisms responsible for the anomalous dysregulation of DUXAP8 in HCC. Transcription factors (TFs) have been extensively documented in the activation of LncRNAs with abnormally high expression levels. Subsequently, we utilized the "HTFtarget" (http://bioinfo.life.hust.edu.cn/hTFtarget#!/) [18] and "PROMO" (https://alggen.lsi.upc.es/cgi-bin/promo v3/promo/promoinit.cgi?dirDB = TF 8.3) [19] to identify putative transcription factors that could

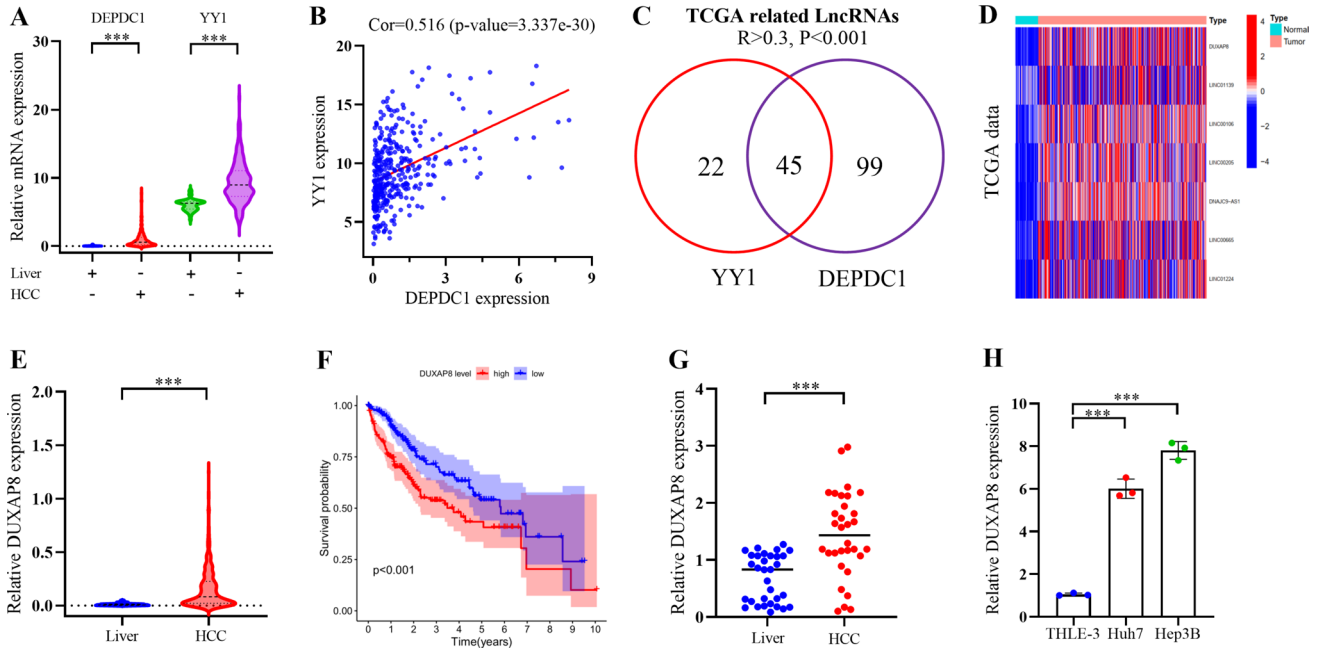

Fig. 1 Identification and characterization of DUXAP8 in HCC tissues and cells. (**A**) The distinct upregulation of YY1 and DEPDC1 in HCC tissues compared to liver tissues obtained by analyzing TCGA-LIHC datasets. (**B**) Expression level of YY1 was significantly correlated with DEPDC1 expression in patients with LIHC of the TCGA database. (**C**) Venn diagram showing the screening of mRNA-specific LncRNAs. A total of 45 LncRNAs were intersected with the LncRNAs co-expressed by YY1 and DEPDC1 (R > 0.3, P < 0.001) in the TCGA-LIHC database. (**D**) Heat maps showing differentially expressed LncRNAs obtained by the TCGA-LIHC database. (**E**) Expression of DUXAP8 in the TCGA-LIHC database. (**F**) The overall survival curve in HCC patients with high or low DUXAP8 expression based on TCGA-LIHC data. (G) The difference expression levels of DUXAP8 between HCC tissues and liver tissues using qRTPCR. (H) qRT-PCR analysis of DUXAP8 levels in two HCC cell lines compared to THLE-3. *p < 0.05, **p < 0.01, ***p < 0.001

Table 2 The HR and P-values of 4 LncRNA

LncRNA	HR	HR.95L	HR.95H	*P*-value	AUC
LINC01011	1.671	1.017	2.744	0.043	0.596
DNAJC9-AS1	1.544	1.167	2.044	0.002	0.639
DUXAP8	1.861	1.210	2.862	0.005	0.680
LINC00205	1.191	1.036	1.370	0.014	0.656

HR and *P*-values were generated from univariate Cox regression in TCGA dataset

potentially bind to the DUXAP8 promoter. These results indicated the presence of two shared transcription factors in both prediction outcomes (Fig. 2A). Therefore, our objective was to examine the precise binding ability of YY1 and VDR to the DUXAP8 promoter and their potential to stimulate its expression. The algorithms utilized by JASPAR (https://jaspar.genereg.net/) [20] to predict YY1 binding sites, that exhibited high predictive scores are shown in Fig. 2B. We assessed the expression of YY1 in THLE-3 cells and in two HCC cell lines that exhibited elevated levels of YY1 expression (Fig. 2C). Subsequently, we individually introduced siRNAs directed toward YY1 (si-YY1) and pcDNA3.1-YY1 into Hep3B cells. Our observations indicated that inhibition of YY1 expression led to a significant decrease in DUXAP8 levels, whereas upregulation of DUXAP8 expression was contingent on YY1 overexpression (Fig. 2D). Chromatin immunoprecipitation assays were performed to demonstrate the binding capacity of YY1 to the DUXAP8 promoter (Fig. 2E). Luciferase assays confirmed that YY1 could bind to the promoter of DUXAP8, as depicted in Fig. 2F. In summary, these data support the notion that YY1 to stimulate the expression of DUXAP8 in hepatocellular carcinoma cells.

DUXAP8 acts as a miR-7-5p sponge

Based on previous findings, DUXAP8 was predominantly expressed in the cytoplasm, leading to the postulation that DUXAP8 could potentially function as an miRNA decoy in HCC. Initially, a cross-analysis was conducted utilizing the microRNA (miRNA) target prediction TargetScan (Release 7.2) [21], StarBase (http://starbase.sysu.edu.cn/) [22], and the lncRNASNP2 (http://bioinfo.life.hust.edu.cn/lncRNASNP/#!/) [23] databases to ascertain the shared miRNAs between DUXAP8 and DEPDC1.We identified three common candidate miRNAs (miR-7-5p, miR-105-5p, and miR-892c-5p) that may bind DUXAP8 and DEPDC1 (Fig. 3A).

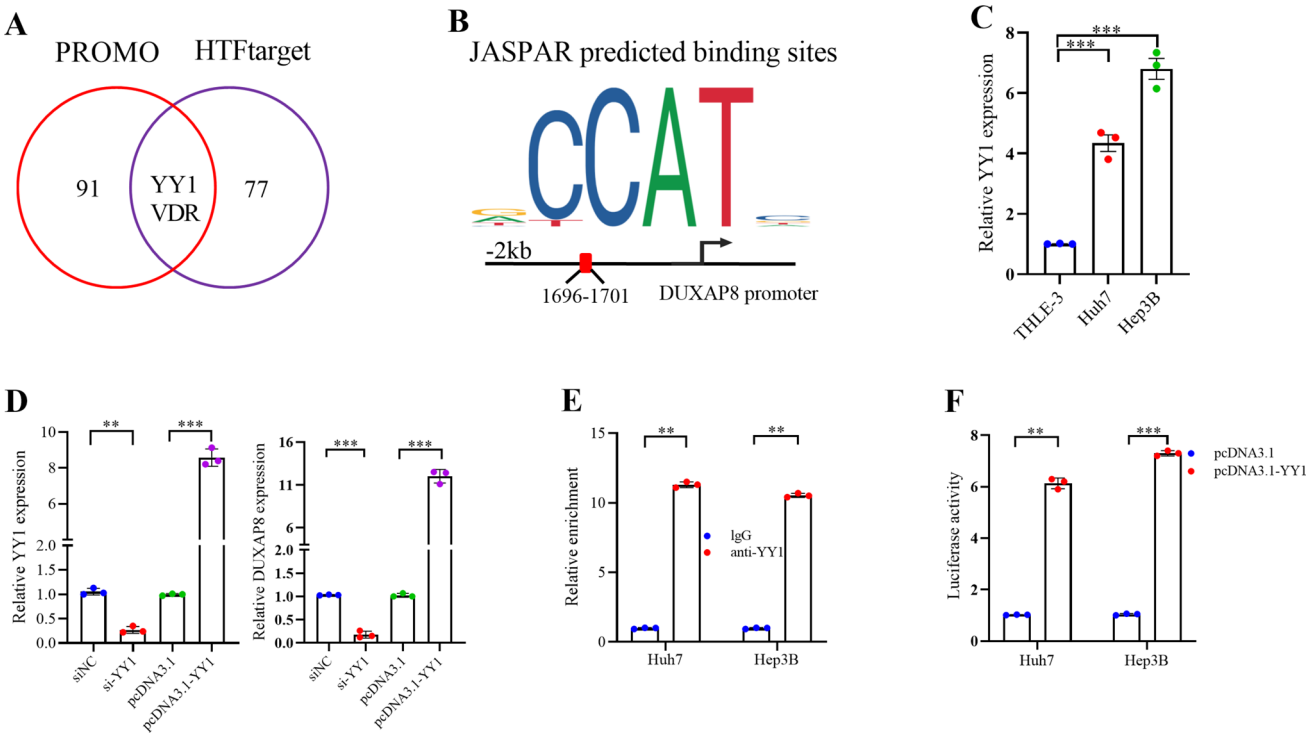

Fig. 2 DUXAP8 is activated by YY1. (**A**) Intersection of HTFtarget and PROMO algorithms predicting the results. (**B**) The JASPAR algorithm predicted the YY1 binding site in DUXAP8 promoter. (**C**) qRT-PCR analysis of YY1 levels in two HCC cell lines compared to THLE-3. (**D**) Real-time PCR measured the levels of YY1 and DUXAP8 in Hep3B cells after various treatments. (**E**) ChIP analyses. (**F**) Luciferase reporter assays. *p < 0.05, **p < 0.01

Next, we evaluated the expression of miR-7-5p, miR-105-5p, and miR-892c-5p in the THLE-3, Huh7, and Hep3B cell lines. The expression of miR-7-5p was reduced in cell lines exhibiting decreased DUXAP8 and DEPDC1 mRNA levels (Fig. 3B). Moreover, the expression of miR-7-5p was elevated in Hep3B and Huh7 cells with DUXAP8 downregulation, whereas it was diminished in Hep3B and Huh7 cells with DUXAP8 overexpression (Fig. 3C).

Subcellular fractionation assays revealed that DUXAP8 and DEPDC1 were predominantly localized in the cytoplasm of Hep3B cells (Fig. 3D). The predicted miRNAs and their binding sites, particularly those linking DUXAP8 and miR-7-5p, are shown in Fig. 3E. To assess the functional correlation between DUXAP8 and miR-7-5p, luciferase assays were performed in HCC cells. Luciferase activity of the luciferase reporter vector containing the DUXAP8 wild-type sequence was significantly reduced upon co-transfection with miR-7-5p mimics in Hep3B cells compared to the controls. However, these inhibitory effects were nullified by mutation of the putative miR-7-5p binding site in DUXAP8, co-transfection with miR-7-5p inhibitor showed the opposite effects (Fig. 3F). Binding was assessed using in vitro-transcribed DUXAP8, which was biotin-labeled, and endogenous miR-7-5p in the cell lysates. These findings confirmed that biotin-labeled DUXAP8 effectively precipitated miR-7-5p (Fig. 3G). miRNAs can bind to their targets, resulting in translational repression and/or RNA degradation in an Ago2 dependent-manner. To determine the regulatory effect of miR-7-5p on DUXAP8, anti-Ago2 RIP was assembled in Hep3B and Huh7 cells that transiently overexpressed miR-7-5p. The enrichment of endogenous DUXAP8 pull-down by Ago2 was observed exclusively in cells transfected with miR-7-5p, thereby indicating that miR-7-5p is a valid miRNA that targets DUXAP8 (Fig. 3H). Therefore, we hypothesized that DUXAP8 functions as a competing endogenous RNA for miR-7-5p in HCC cells.

DUXAP8 functions as a ceRNA

To determine the effect of miR-7-5p on DEPDC1 expression, an initial assessment of DEPDC1 and DUXAP8 mRNA levels was conducted following miR-7-5p overexpression or knockdown. These findings indicate that miR-7-5p significantly reduced the mRNA expression of DEPDC1 and

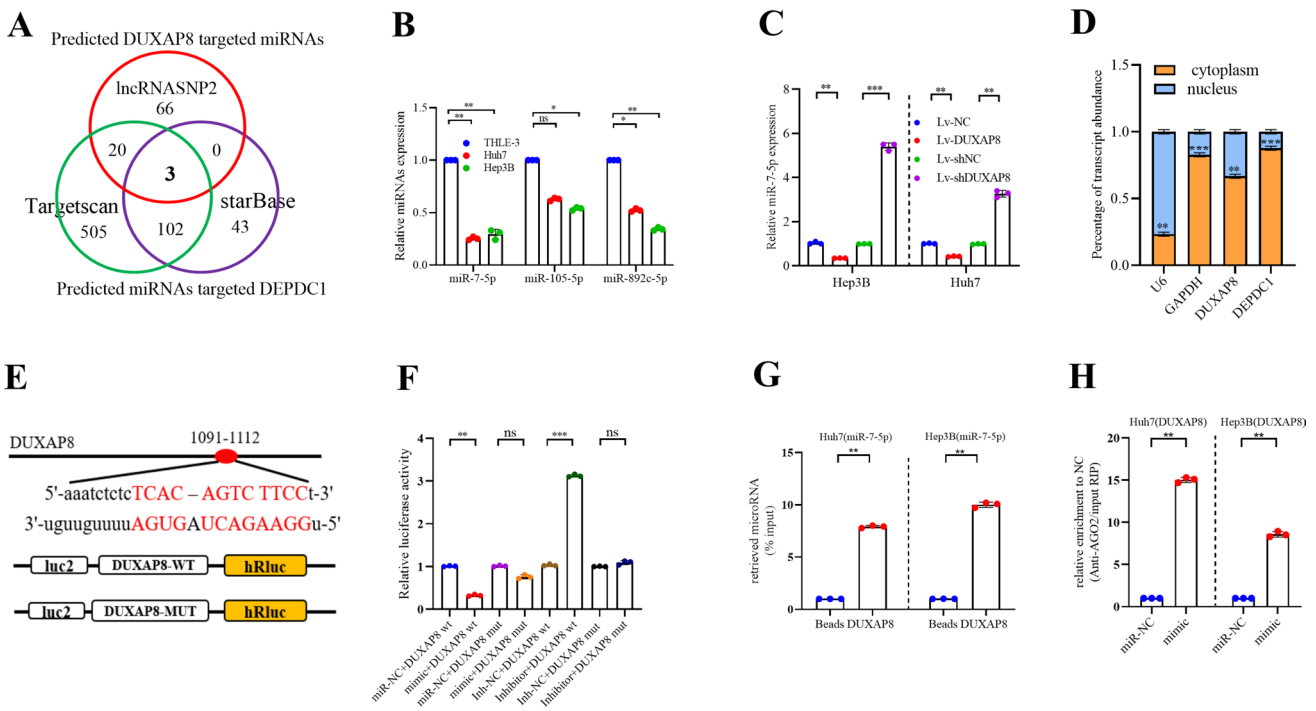

Fig. 3 DUXAP8 directly targets miR-7-5p. (**A**) Venn diagram showing the potential miRNAs that target both DEPDC1 and DUXAP8 were predicted using the lncRNASNP2, TargetScan and starbase databases. (**B**) The expression levels of the miRNAs in THLE-3 、Hep3B and Huh7 cells. (**C**) The mRNA levels of miR-7-5p in Hep3B and Huh7 cells after transfection with Lv-DUXAP8 or Lv-shDUXAP8. (**D**) Localization of DUXAP8 and DEPDC1 was assessed by qRTPCR in Hep3B and Huh7 cells. U6 and GAPDH were used as positive controls for nuclear RNA and cytoplasmic RNA, respectively. (**E**) Binding sequences of DUXAP8 and miR-7-5p based on bioinformatics analysis and schematic constructions of WT-Luc (DUXAP8 3′ partial region), MUT-Luc. (**F**) Luciferase activity assays were performed cotransfected with DUXAP8 WT or DUXAP8 MUT and miR-7-5p mimic or inhibitor. (**G**) HCC cell lysates were incubated with biotin-labeled DUXAP8, miRNA qRT-PCR was performed after the pull-down process. (H) Anti-AGO2 RIP was performed in Hep3B and Huh7 cells transfected with miR-7-5p mimics or miR-NC, followed by qRT-PCR to detect DUXAP8 enrichment. Data are shown as mean ± SD, n = 3. The data statistical significance is assessed by Student's t test. *P < 0.05, **P <0.01, ***P < 0.001

DUXAP8 in Hep3B and Huh7 cells, whereas the miR-7-5p inhibitor significantly elevated the mRNA levels of DEPDC1 and DUXAP8 (Fig. 4A–C). To corroborate the association between DEPDC1 and its corresponding miRNAs, an examination using TargetScan (Release 7.2) demonstrated the presence of anticipated miR-7-5p targeting sites in DEPDC1(Fig. 4D). The results of luciferase reporter assays indicated that the expression of luciferase under the regulation of wild-type DEPDC1 was considerably suppressed in Hep3B cells upon co-transfection with the miR-7-5p mimic compared to that in the control group. The inhibitory effect was nullified when the one putative miR-7-5p binding sites located in the DEPDC1 3′UTR were mutated. Conversely, co-transfection with miR-7-5p inhibitor resulted in the opposite effect (Fig. 4E). Collectively, these findings demonstrated that DEPDC1 is targeted by miR-7-5p.

A previous study has demonstrated that DUXAP8 is involved in Ago2-associated RNA-induced silencing complexes (RISCs) and interacts with miRNAs. The present study investigated the correlation between DUXAP8 and DEPDC1 mRNA in RISCs through RNA immunoprecipitation (RIP) using an anti-Ago2 antibody, followed by quantitative real-time polymerase chain reaction (qRT-PCR). Cytoplasmic enrichment of DUXAP8 and DEPDC1 mRNA in the Ago2 complexes is shown in Fig. 4F. Significantly reduced levels were observed in the Ago2 complexes isolated from the nucleus. These findings provided additional evidence that DUXAP8 functions as a ceRNA for DEPDC1 mRNA in the cytoplasm. Furthermore, RIP assays utilizing Ago2, a protein capable of selectively enriching miRNA-bound targets through immunoprecipitation. DUXAP8 was independently overexpressed in Hep3B and Huh7 cells, followed by the use of an anti-Ago2 antibody to pull down Ago2. Overexpression of DUXAP8 resulted in a notable reduction in the enrichment of DEPDC1 transcripts pulled down by Ago2, thereby indicating a decrease in the abundance of miRNA-bound DEPDC1 transcripts (Fig. 4G). To determine the potential role of DUXAP8 as a ceRNA in the regulation of DEPDC1 via miR-7-5p, luciferase assays were conducted using the pGL3-promoter-DEPDC1 in HCC cells.

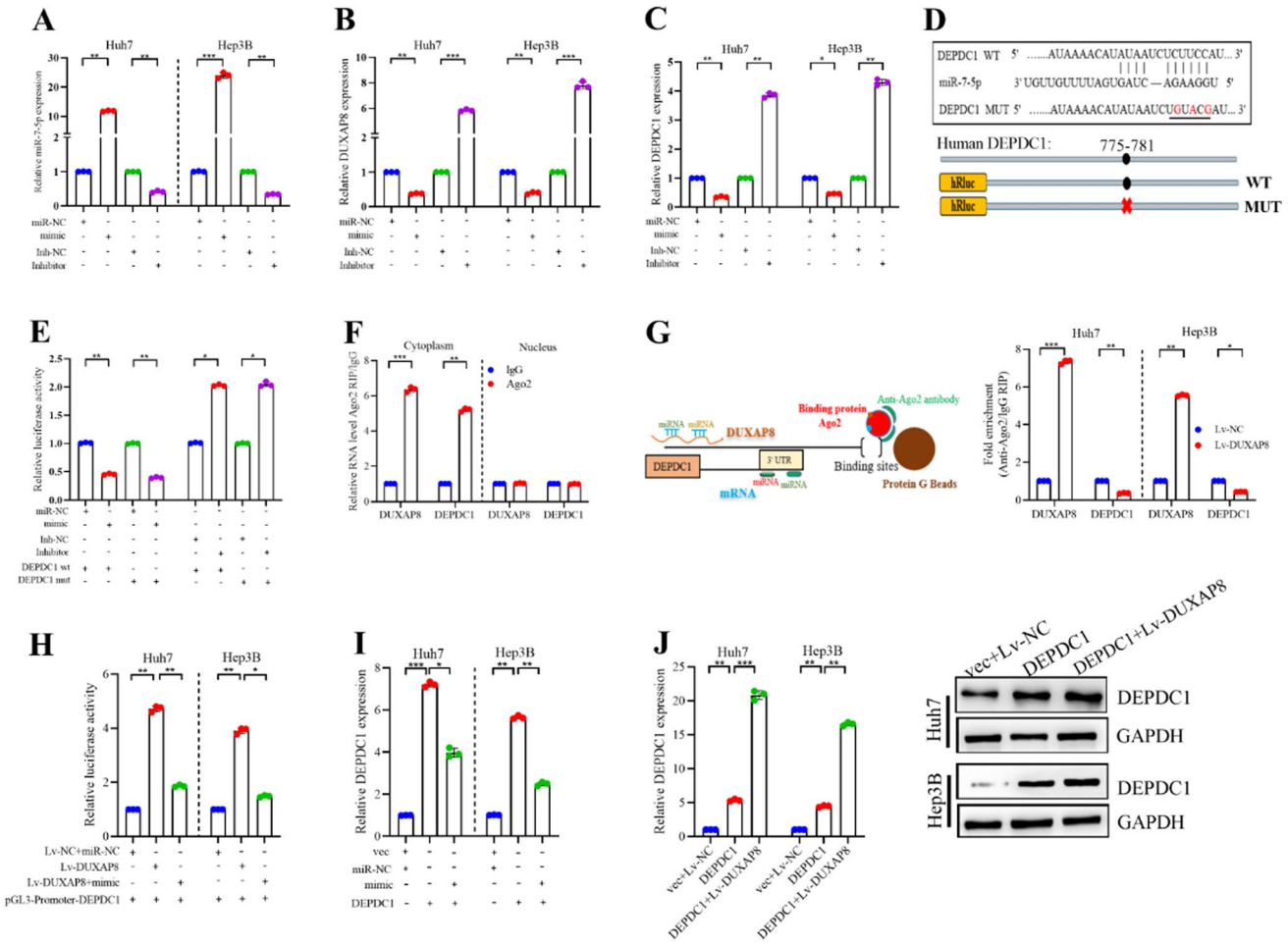

Fig. 4 DUXAP8 act as ceRNAs. (**A**) The qRT-PCR assay revealed the overexpression and knockdown efficiency of miR-7-5p in Hep3B and Huh7 cells. (**B**–**C**) The mRNA levels of DUXAP8 and DEPDC1 in Hep3B and Huh7 cells after transfection with miR-7-5p mimic or Inhibitor. (**D**) The miR-7-5p binding sequence in the DEPDC1 3′ UTR and the generation of dual-luciferase reporter plasmids of wild-type (WT) or mutant (MUT) were shown. (**E**) Luciferase activity assays were performed in Hep3B cells co-transfected with DEPDC1 WT or MUT and miR-7-5p mimic or inhibitor. (**F**) RIP experiments revealed that DUXAP8 and DEPDC1 mRNA coexisted in the anti-Ago2 complex in the cell cytoplasm. IgG was used as the negative control. (**G**) The schematic diagram and qRT-PCR results of the RIP based on Ago2 showed that DUXAP8 can compete with the DEPDC1 transcript for the binding of miRNAs. (**H**) Luciferase activity in HCC cells co-transfected with pGL3-promoter-DEPDC1 and ceRNAs. Data were presented as the relative ratio of renilla luciferase activity and firefly luciferase activity. (**I**) The relative expressions of DEPDC1 were determined transfected with miR-7-5p mimic or DEPDC1 by qRT-PCR. (**J**) The relative expression levels of DEPDC1 were determined by qRT-PCR and western blotting in Hep3B and Huh7 cells after co-transfecting ceRNAs. Data are shown as mean ± SD, n = 3. The data statistical significance is assessed by Student's t test. *P < 0.05, **P < 0.01, ***P < 0.001

Upregulation of DUXAP8 resulted in a significant increase in luciferase activity of the reporter, which was effectively nullified upon co-transfection with the miR-7-5p mimic (Fig. 4H). To confirm the association between DEPDC1 and miR-7-5p, the upregulation of DEPDC1 was inhibited by miR-7-5p overexpression (Fig. 4I). This finding implied that DUXAP8 has the potential to compete with DEPDC1 transcripts for miRNA binding. Subsequently, we induced DUXAP8 overexpression in cells that were previously overexpressing DEPDC1. As demonstrated above, upregulation of DEPDC1 by DEPDC1 further enhanced the expression of DEPDC1 at both the transcriptional and translational levels through the involvement of DUXAP8 (Fig. 4J). Collectively, these findings suggested that DUXAP8 acts as a ceRNA to antagonize miR-7-5p, thereby enhancing the expression of DEPDC1.

The expression of HNRNPF is regulated by DUXAP8

To expand the investigation into additional mechanisms by which DUXAP8 governs DEPDC1, we searched for protein-binding associates of DUXAP8. Because biotin-labeled

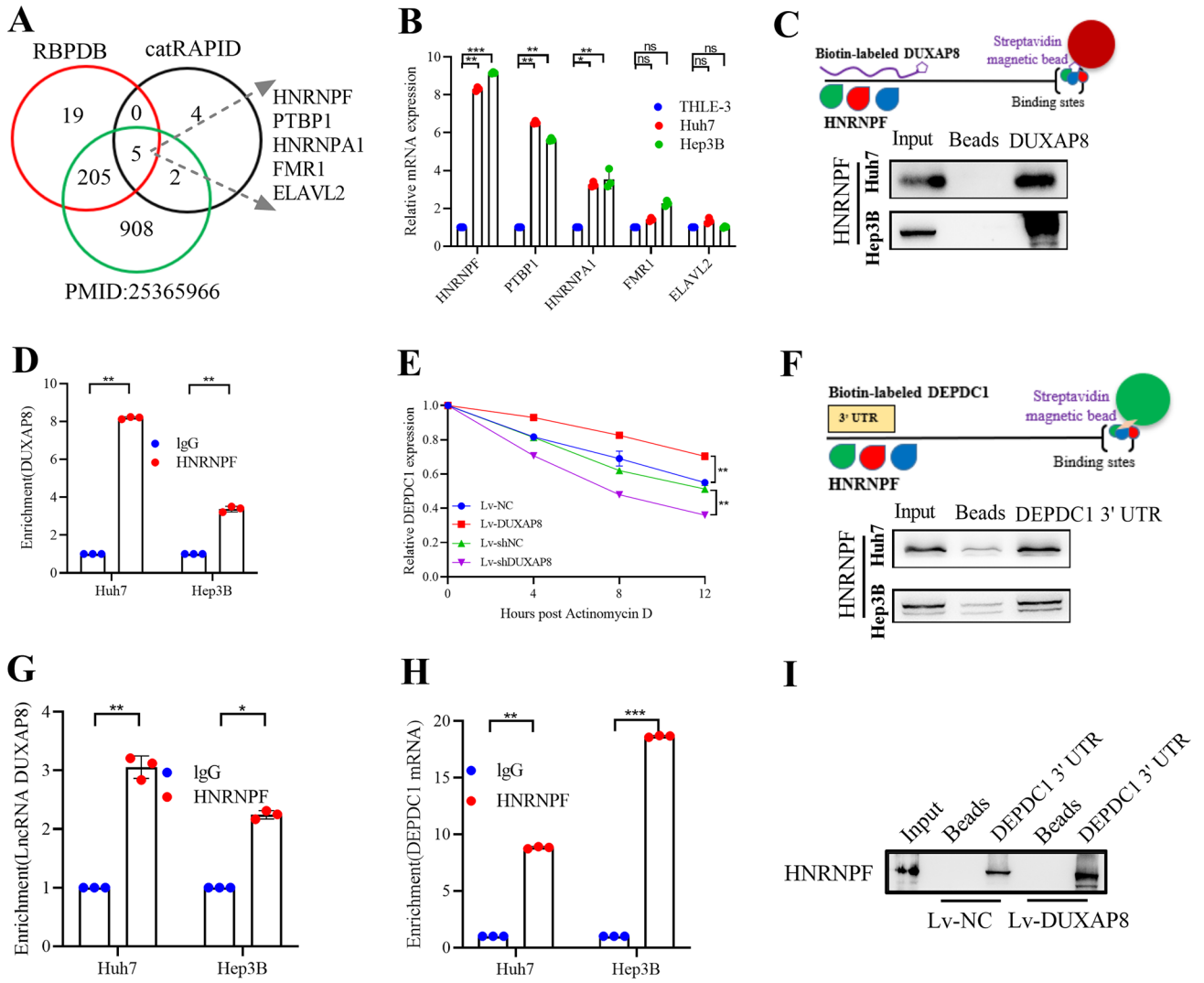

Fig. 5 DUXAP8 specifically regulates DEPDC1 by facilitating the interaction of HNRNPF with DEPDC1 mRNA. (**A**) Venn diagram showing the RNA-binding protein shared in RBPDB, catRAPID database and PMID:25365966. (**B**) The expression levels of the mRNAs in THLE-3、Hep3B and Huh7 cells. (**C**) The schematic diagram of the RNA pull-down method used to identify the binding between DUXAP8 and RBP in both Hep3B and Huh7 cells; interaction of DEPDC1 with HNRNPF, as detected by RNA precipitation using DEPDC1 as an RNA probe, followed by western blot. (**D**) RIP assay using HNRNPF antibody confirms that DEPDC1 interacts with HNRNPF. (**E**) Increase of DEPDC1 mRNA stability after transfection Lv-DUXAP8, re-expression of Lv-shDUXAP8 restores its ability to decrease DEPDC1 mRNA stability as compared to control cells. Cells were treated with 2.5 μg/mL actinomycin D and RNA was isolated at 0, 4, 8 and 12 h, respectively. (**F**) The schematic diagram of the RNA pull-down method used to identify the binding between DEPDC1 and RBP in both Hep3B and Huh7 cells; interaction of DEPDC1 with HNRNPF, as detected by RNA precipitation using DEPDC1 as an RNA probe, followed by western blot. (**G**) RIP assay using HNRNPF antibody confirms that DEPDC1 interacts with HNRNPF. (**H**) DUXAP8 is required for the interaction of HNRNPF with DEPDC1 mRNA, as detected by RIP assay using HNRNPF antibody. (**I**) DUXAP8 enhances the interaction of DEPDC1 mRNA with HNRNPF, as detected by RNA precipitation using DEPDC1 3′-UTR probe. Data are shown as mean ± SD, n = 3. The data statistical significance is assessed by Student's t test. *P < 0.05, **P < 0.01, ***P < 0.001

DUXAP8 was used as a probe, we performed RNA precipitation and identified several prospective binding partners for DUXAP8. Four RNA-binding proteins (RBPs) were identified using the RBPDB (http://rbpdb.ccbr.utoronto.ca/) [24] and catRAPID (http://service.tartaglialab.com/page/catrapid_group) [25] databases, as reported in the literature on human RBPs (Fig. 5A). Next, we evaluated the expression of HNRNPF, PTBP1, HNRNPA1, FMR1, and ELAVL2 in THLE-3, Huh7, and Hep3B cell lines and found that HNRNPF expression was higher in these cell lines (Fig. 5B). The interaction between HNRNPF and DUXAP8 in Hep3B and Huh7 cells was confirmed using western blot analysis (Fig. 5C). The presence of DUXAP8 in the HNRNPF

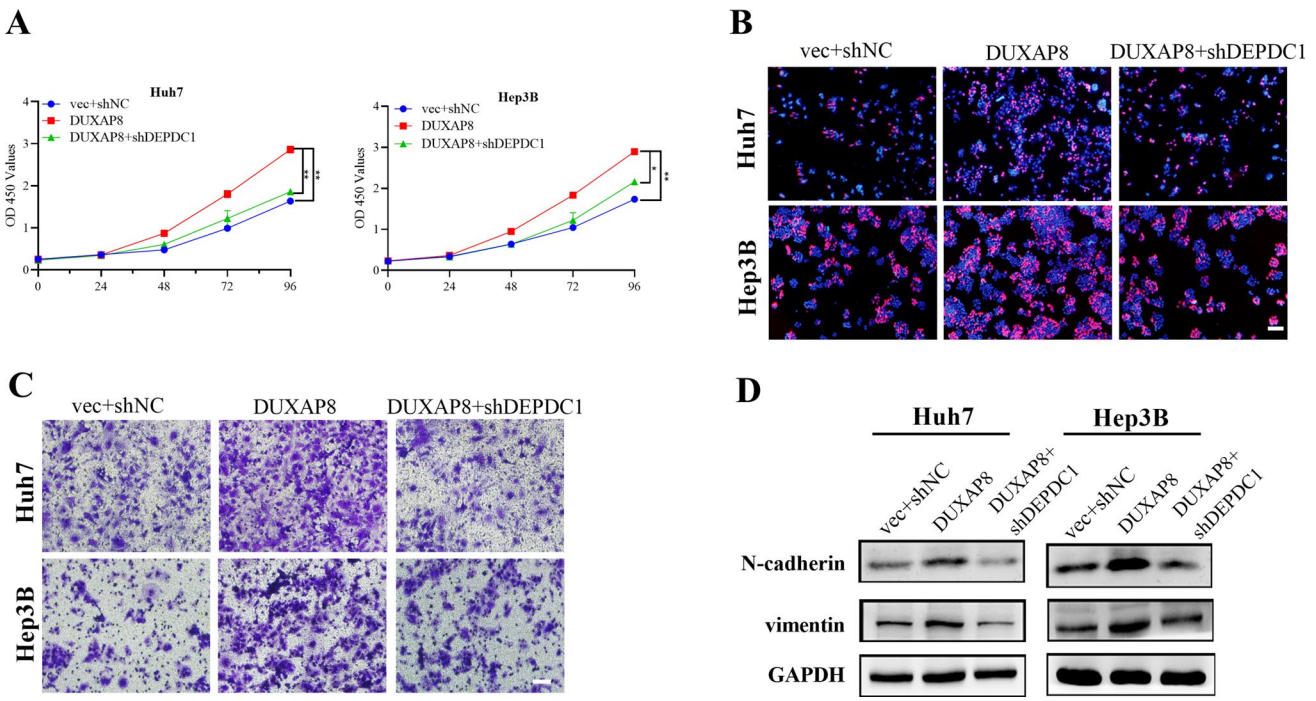

Fig. 6 DUXAP8 increased the progression via DEPDC1 in HCC cells. (**A**) Cell proliferation was assessed daily for 4 days using the Cell Counting Kit-8 (CCK-8) assay in DUXAP8 overexpressing Hep3B and Huh7 cells. (**B**) EdU assays were performed to analyze the Hep3B and Huh7 cell proliferation in differently transfected groups. (**C**) Transwell assays were used to evaluate the involvement of DUXAP8 for invasion in DUXAP8 overexpressing Hep3B and Huh7 cells. (**D**) Western blotting detected the protein levels of N-cadherin and vimentin in Hep3B and Huh7 cells. Data are shown as mean ± SD, n = 3. The data statistical significance is assessed by Student's t test. *P < 0.05, **P < 0.01, ***P < 0.001

complexes was confirmed using RIP assays using an antibody against HNRNPF and compared to the IgG control. This finding provided additional evidence that HNRNPF is a binding partner of DUXAP8 (Fig. 5D). Previous studies have demonstrated that HNRNPF enhances the stability of downstream genes. Consequently, our initial investigation aimed to assess the potential impact of DUXAP8 on the stability of DEPDC1 mRNA. Previous studies have demonstrated that HNRNPF enhances the stability of downstream genes. As a preliminary step, we investigated the potential influence of DUXAP8 on the stability of DEPDC1 mRNA. Cells were treated with the RNA synthesis inhibitor actinomycin D, followed by the isolation of total RNA at 4, 8, and 12 h. The data indicated that the expression of DUXAP8 resulted in an increase in the stability of DEPDC1 mRNA, whereas inhibition of DUXAP8 expression led to a decrease in the stability of DEPDC1 mRNA (Fig. 5E). The results of this study suggest that DUXAP8 plays a role in augments the stability of DEPDC1 mRNA.

To elucidate the mechanism by which DUXAP8 modulates the stability of DEPDC1 mRNA through its interaction with HNRNPF, RNA precipitation assays were conducted in Hep3B and Huh7 cells using DEPDC1 3′-UTR mRNA as a probe, which demonstrated the interaction between

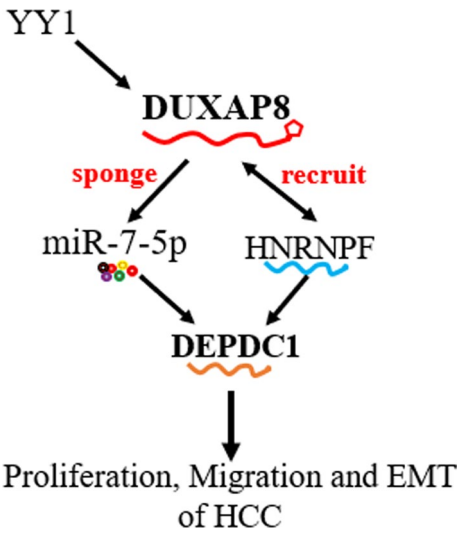

Fig. 7 The schematic model of DUXAP8 functions

HNRNPF and DEPDC1 mRNA (Fig. 5F). Utilization of the HNRNPF antibody in RIP experiments showed an increase in DUXAP8 within the HNRNPF complexes (Fig. 5G).

Table 3 Correlation between the clinicopathologic characteristics of the patients with hepatocellular carcinoma and the expression of YY, DUXAP8 and DEPDC1

Characteristics	n	YY1			DUXAP8			DEPDC1		
		High	Low	*P*-value	High	Low	*P*-value	High	Low	*P*-value
Gender										
Male	28	12	16	0.496	18	10	0.581	15	13	0.419
Female	04	01	03		02	02		03	01	
Age (years)										
≥60	06	04	02	0.687	03	03	0.865	02	04	0.102
<60	26	15	11		12	14		18	08	
Differentiation										
Poorly	28	13	15	0.419	08	20	0.387	11	17	0.178
Moderate/well	04	01	03		02	02		03	01	
Clinical stage										
I–II	08	03	05	**0.028***	02	06	**0.002***	01	07	**0.004****
III–IV	24	19	05		20	04		17	07	
Hepatitis B										
Negative	09	02	07	0.125	03	06	**0.016***	05	04	0.053
Positive	23	12	11		18	05		20	03	
Pathological										
HCC	25	18	07	**0.036***	20	05	**0.009****	19	06	**0.003****
Other types	07	02	05		02	05		01	06	
Tumor size										
≥6 cm	21	08	13	0.373	10	11	0.174	16	05	0.082
<6 cm	11	06	05		08	03		05	06	

YY1 Yin Yang 1, *DEPDC1* DEP domain containing 1, *DUXAP8 LncRNA* double homeobox A pseudogene 8, *HCC* hepatocellular carcinoma.*$P < 0.05$, **$P < 0.01$, ***$P < 0.001$

Furthermore, our findings indicate that DUXAP8 modulates the interaction between HNRNPF and DEPDC1 mRNA. The results indicated that DUXAP8 overexpression led to a significant increase in the enrichment of DEPDC1 mRNA within HNRNPF complexes compared to that in control cells (Fig. 5H). These findings suggest that DUXAP8 promotes the interaction between HNRNPF and DEPDC1 mRNA. Our hypothesis was reinforced by RNA precipitation using the DEPDC1 3′-UTR mRNA probe. In our study, we observed a marginal increase in the quantity of HNRNPF that was bound to the DEPDC1 3′-UTR mRNA probe in cells that overexpressed DUXAP8, as compared to cells in the control group (Fig. 5I). This finding provides additional evidence to support the notion that DUXAP8 facilitates the interaction between HNRNPF and DEPDC1 mRNA.

DUXAP8 promotes the proliferation and migration of HCC cells in vitro

Subsequently, we investigated the effects of DUXAP8 on the cellular phenotypes. The study revealed that overexpression of DUXAP8 led to a noteworthy enhancement in the proliferative capacity of Hep3B and Huh7 cells, as evidenced by the results of the Cell Counting Kit-8 (Fig. 6A) and EdU (Fig. 6B) assays. However, this increase was abolished by the transfection with shDEPDC1. The results of the Transwell experiments indicated that overexpression of DUXAP8 led to a noteworthy enhancement in the migratory ability of HCC cells. However, this effect was partially mitigated by transfection with shDEPDC1 (Fig. 6C). Furthermore, the progression of epithelial-mesenchymal transition (EMT) is characterized by an increase in the expression of mesenchymal cell markers, including N-cadherin and vimentin. Western blot analysis indicated that overexpression of DUXAP8 led to a significant increase in the expression of N-cadherin and vimentin in both Hep3B and Huh7 cells. This increase was partially alleviated upon transfection with shDEPDC1 (Fig. 6D). Collectively, these data indicate that DUXAP8 plays a functional role in the initiation of endothelial-mesenchymal transition, which is contingent upon the expression of DEPDC1.

Discussion

Evidence suggests that cytoplasmic lncRNAs function as miRNA sponges, leading to the aberrant activity of miRNAs and their target genes. Additionally, they modulate tumorigenesis by interacting with RBPs [7, 16]. YY1 and

DEPDC1 are considered among the most significant oncogenes, as their activation results in the controlled expression of numerous target genes, ultimately culminating in cancer development [26, 27]. Multiple mechanisms contribute to DEPDC1 upregulation, including transcriptional activation [28, 29] and posttranscriptional regulation [30, 31]. A significantly upregulated prognosis-related lncRNA, DUXAP8, was identified in HCC tissues and cells using bioinformatic analyses and a series of validation experiments. Moreover, it has been reported that activation of DUXAP8 by YY1 contributes to the progression of HCC through competitive binding with miR-7-5p and upregulation of DEPDC1 mRNA, leading to the induction of EMT. The upregulation of DEPDC1 expression was partially attributed to its ability to enhance the stability of DEPDC1 mRNA through its interaction with HNRNPF. Thus, the significance of DUXAP8 in HCC progression was noteworthy (Fig. 7).

Our findings indicate a potential association between DUXAP8 and DEPDC1. This study revealed the presence of miR-7-5p response elements in both DUXAP8 and DEPDC1 mRNA. Overexpression of DUXAP8 resulted in an mRNA expression profile that further supports its involvement in the advancement of hepatocellular progression. The involvement of DUXAP8 in HCC was attributed to its competitive binding to miR-7-5p, indicating its role as a ceRNA. The upregulation of DEPDC1 by DUXAP8 may enhance its effects due to the existence of a negative feedback loop between miR-7-5p and DEPDC1. To elucidate the precise function of DUXAP8, HNRNPF, and DEPDC1 in HCC tissues, we investigated the correlation between YY1, DUXAP8, HNRNPF, and DEPDC1 mRNA expression and clinicopathological parameters of patients with HCC, as presented in Table 3. Correlation regression analysis indicated a statistically significant association between elevated YY1 expression and clinical stage ($P=0.028$) and pathological stage ($P=0.036$), whereas DUXAP8 expression correlated with clinical stage ($P=0.002$), pathological stage ($P=0.009$), and hepatitis B ($P=0.016$), and DEPDC1 expression correlated with clinical stage ($P=0.004$) and pathological stage ($P=0.003$). The data presented herein provide evidence of a significant correlation between elevated levels of YY1, DUXAP8, and DEPDC1 and the occurrence of HCC.

In summary, this study revealed the oncogenic mechanism of DUXAP8 in HCC. Regulation of DUXAP8 activation by YY1 on DEPDC1 involves the maintenance of DEPDC1 mRNA stability and the function of DUXAP8 as a competing endogenous RNA. Our findings indicate that the expression of DUXAP8 is increased in HCC. Moreover, DUXAP8 interacts with HNRNPF, promoting the association of HNRNPF with DEPDC1 mRNA and stabilizing DEPDC1 mRNA levels. Additionally, our findings demonstrated that the involvement of DUXAP8 in HCC progression is facilitated by YY1. The modulation of DEPDC1 expression, which contributes to HCC progression, is facilitated by the interaction between DUXAP8 sponges and miR-7-5p. The multifaceted effect of DUXAP8 on HCC progression indicates that DUXAP8 may serve as a promising therapeutic target for patients with HCC.

Acknowledgements We appreciate the technical supports of lab members.

Author contributions YC and CT: conception and design of the study and manuscript writing; experiments; data analysis; YS and NL: bioinformatics analysis and result interpretation; All authors read and approved the final manuscript.

Funding The work was supported by grants from the National Natural Science Foundation of China (Nos. 82360539); the Cultivation Project of Guizhou Medical University Affiliated Hospital (gyfynsfc [2020]-17, gyfynsfc [2022]-12); Science and Technology Planning Project of Guizhou Province (qkhjc-zk [2022]-yb435) and the Affiliated Hospital of Guizhou Medical University Doctoral Research Startup Fund [gyfybsky-2022-48].

Data availability No datasets were generated or analyzed during the current study.

Declarations

Competing interests The authors declare no competing interests.

Ethics approval and consent to participate This study was approved by the Ethics Committee of Affiliated Hospital of Guizhou Medical University. All enrolled participants gave written informed consent to participate and publish in accordance with the Declaration of Helsinki.

Consent for publication Not applicable.

References

1. Siegel RL, Miller KD, Fuchs HE, Jemal A. Cancer statistics, 2021. CA Cancer J Clin. 2021;71(1):7–33. https://doi.org/10.3322/caac.21654.
2. Kulik L, El-Serag HB. Epidemiology and management of hepatocellular carcinoma. Gastroenterology. 2019;156(2):477-491.e1. https://doi.org/10.1053/j.gastro.2018.08.065.

3. Vogel A, Meyer T, Sapisochin G, Salem R, Saborowski A. Hepatocellular carcinoma. Lancet. 2022;400(10360):1345–62. https://doi.org/10.1016/S0140-6736(22)01200-4.
4. Torimura T, Iwamoto H. Treatment and the prognosis of hepatocellular carcinoma in Asia. Liver Int. 2022;42(9):2042–54. https://doi.org/10.1111/liv.15130.
5. Li Y, Tian Y, Zhong W, Wang N, Wang Y, Zhang Y, Zhang Z, Li J, Ma F, Zhao Z, Peng Y. Artemisia Argyi essential oil inhibits hepatocellular carcinoma metastasis via suppression of DEPDC1 dependent Wnt/β-catenin signaling pathway. Front Cell Dev Biol. 2021;29(9): 664791. https://doi.org/10.3389/fcell.2021.664791.
6. Zhou C, Wang P, Tu M, Huang Y, Xiong F, Wu Y. DEPDC1 promotes cell proliferation and suppresses sensitivity to chemotherapy in human hepatocellular carcinoma. Biosci Rep. 2019;39(7):BSR201909646. https://doi.org/10.1042/BSR20190946.
7. Tian C, Abudoureyimu M, Lin X, Chu X, Wang R. Linc-ROR facilitates progression and angiogenesis of hepatocellular carcinoma by modulating DEPDC1 expression. Cell Death Dis. 2021;12(11):1047. https://doi.org/10.1038/s41419-021-04303-5.
8. Li YY, Li W, Chang GZ, Li YM. Long noncoding RNA KTN1 antisense RNA 1exerts an oncogenic function in lung adenocarcinoma by regulating DEP domain containing 1 expression via activating epithelial-mesenchymal transition. Anticancer Drugs. 2021;32(6):614–25. https://doi.org/10.1097/CAD.0000000000001035.
9. Li Y, Hu J, Guo D, Ma W, Zhang X, Zhang Z, Lu G, He S. LncRNA SNHG5 promotes the proliferation and cancer stem cell-like properties of HCC by regulating UPF1 and Wnt-signaling pathway. Cancer Gene Ther. 2022;29(10):1373–83. https://doi.org/10.1038/s41417-022-00456-3.
10. Bartonicek N, Maag JL, Dinger ME. Long noncoding RNAs in cancer: mechanisms of action and technological advancements. Mol Cancer. 2016;15(1):43. https://doi.org/10.1186/s12943-016-0530-6.
11. Biferali B, Mocciaro E, Runfola V, Gabellini D. Long non-coding RNAs and their role in muscle regeneration. Curr Top Dev Biol. 2024;158:433–65. https://doi.org/10.1016/bs.ctdb.2024.02.010.
12. Meng J, Han J, Wang X, et al. Twist1-YY1-p300 complex promotes the malignant progression of HCC through activation of miR-9 by forming phase-separated condensates at super-enhancers and relieved by metformin. Pharmacol Res. 2023;188:106661. https://doi.org/10.1016/j.phrs.2023.106661.
13. Herman AB, Tsitsipatis D, Gorospe M. Integrated lncRNA function upon genomic and epigenomic regulation. Mol Cell. 2022;82(12):2252–66. https://doi.org/10.1016/j.molcel.2022.05.027.
14. Yip CW, Sivaraman DM, Prabhu AV, Shin JW. Functional annotation of lncRNA in high-throughput screening. Essays Biochem. 2021;65(4):761–73. https://doi.org/10.3390/vaccines11101593.
15. Wang B, Xu W, Cai Y, Chen J, Guo C, Zhou G, Yuan C. DUXAP8: a promising lncRNA with carcinogenic potential in cancer. Curr Med Chem. 2022;29(10):1677–86. https://doi.org/10.2174/0929867328666210726092020.
16. Yu Hu, Zhang X, Zai H-Y, Jiang W, Xiao L, Zhu Q. lncRNA DUXAP8 facilitates multiple malignant phenotypes and resistance to PARP inhibitor in HCC via upregulating FOXM1. Mol Ther Oncolytics. 2020;16(19):308–22. https://doi.org/10.1016/j.omto.2020.10.010.
17. Blum A, Wang P, Zenklusen JC. SnapShot: TCGA-analyzed tumors. Cell. 2018;173(2):530. https://doi.org/10.1016/j.cell.2018.03.059.
18. Zhang Q, Liu W, Zhang HM, Xie GY, Miao YR, Xia M, Guo AY. hTFtarget: a comprehensive database for regulations of human transcription factors and their targets. Genomics Proteomics Bioinform. 2020;18(2):120–8. https://doi.org/10.1016/j.gpb.2019.09.006.
19. Netanely D, Stern N, Laufer I, Shamir R. PROMO: an interactive tool for analyzing clinically-labeled multi-omic cancer datasets. BMC Bioinform. 2019;20(1):732. https://doi.org/10.1186/s12859-019-3142-5.
20. Castro-Mondragon JA, Riudavets-Puig R, Rauluseviciute I, Lemma RB, Turchi L, Blanc-Mathieu R, Lucas J, Boddie P, Khan A, Manosalva Pérez N, Fornes O, Leung TY, Aguirre A, Hammal F, Schmelter D, Baranasic D, Ballester B, Sandelin A, Lenhard B, Vandepoele K, Wasserman WW, Parcy F, Mathelier A. JASPAR 2022: the 9th release of the open-access database of transcription factor binding profiles. Nucleic Acids Res. 2022;50(D1):D165–73. https://doi.org/10.1093/nar/gkab1113.
21. Górecki I, Rak B. The role of microRNAs in epithelial to mesenchymal transition and cancers; focusing on mir-200 family. Cancer Treat Res Commun. 2021;28: 100385. https://doi.org/10.1016/j.ctarc.2021.100385.
22. Li JH, Liu S, Zhou H, Qu LH, Yang JH. starBase v2.0: decoding miRNA-ceRNA, miRNA-ncRNA and protein-RNA interaction networks from large-scale CLIP-Seq data. Nucleic Acids Res. 2014;42:D92–7. https://doi.org/10.1093/nar/gkt1248.
23. Miao YR, Liu W, Zhang Q, Guo AY. lncRNASNP2: an updated database of functional SNPs and mutations in human and mouse lncRNAs. Nucleic Acids Res. 2018;46(D1):D276–80. https://doi.org/10.1093/nar/gkx1004.
24. Cook KB, Kazan H, Zuberi K, Morris Q, Hughes TR. RBPDB: a database of RNA-binding specificities. Nucleic Acids Res. 2011;39:D301–8. https://doi.org/10.1093/nar/gkq1069.
25. Armaos A, Colantoni A, Proietti G, Rupert J, Tartaglia GG. catRAPID omics v2.0: going deeper and wider in the prediction of protein-RNA interactions. Nucleic Acids Res. 2021;49(W1):W72–9. https://doi.org/10.1093/nar/gkab393.
26. Wang W, Li D, Sui G. YY1 is an inducer of cancer metastasis. Crit Rev Oncog. 2017;22(1–2):1–11. https://doi.org/10.1615/CritRevOncog.2017021314.
27. Shi J, Hao A, Zhang Q, Sui G. The role of YY1 in oncogenesis and its potential as a drug target in cancer therapies. Curr Cancer Drug Targets. 2015;15(2):145–57. https://doi.org/10.2174/1568009615666150131124200.
28. Wang W, Li A, Han X, Wang Q, Guo J, Wu Y, Wang C, Huang G. DEPDC1 up-regulates RAS expression to inhibit autophagy in lung adenocarcinoma cells. J Cell Mol Med. 2020;24(22):13303–13. https://doi.org/10.1111/jcmm.15947.
29. Shen L, Li H, Liu R, Zhou C, Bretches M, Gong X, Lu L, Zhang Y, Zhao K, Ning B, Yang SY, Zhang A. DEPDC1 as a crucial factor in the progression of human osteosarcoma. Cancer Med. 2023;12(5):5798–808. https://doi.org/10.1002/cam4.5340.
30. Gong Z, Chu H, Chen J, Jiang L, Gong B, Zhu P, Zhang C, Wang Z, Zhang W, Wang J, Li C, Zhao H. DEPDC1 upregulation promotes cell proliferation and predicts poor prognosis in patients with gastric cancer. Cancer Biomark. 2021;30(3):299–307. https://doi.org/10.3233/CBM-201760.
31. Qiu J, Tang Y, Liu L, Yu J, Chen Z, Chen H, Yuan R. FOXM1 is regulated by DEPDC1 to facilitate development and metastasis of oral squamous cell carcinoma. Front Oncol. 2022;22(12): 815998. https://doi.org/10.3389/fonc.2022.815998.